Discussion: "Isotropic Clamped-Free Thin Annular Circular Plate Subjected to a Concentrated Load" (Adewale, A. O., 2006, ASME J. Appl. Mech., 73, pp. 658–663)

J. T. Chen
Department of Harbor and River Engineering,
National Taiwan Ocean University,
Keelung 20224, Taiwan, R.O.C.
e-mail: jtchen@mail.ntou.edu.tw

W. M. Lee
Department of Mechanical Engineering,
China Institute of Technology,
Taipei 11581, Taiwan, R.O.C.
e-mail: wmlee@cc.chit.edu.tw

H. Z. Liao
Department of Harbor and River Engineering,
National Taiwan Ocean University,
Keelung 20224, Taiwan, R.O.C.

1 Introduction

In this interesting paper [1], a concentrated load was applied to the clamped-free annular plate. The problem domain was divided into two parts by the cylindrical section where a concentrated load was applied. The author used the Trefftz method [2] to construct the homogeneous solution

$$u = \sum_{m=0}^{\infty} R_m(r)\cos m\theta \tag{1}$$

in each part. By substituting Eq. (1) into the governing equation, the author could determine $R_m(r)$. Mathematically speaking, the series in Eq. (1) can be seen as the summation of Trefftz bases. To simulate the concentrated force, a circularly distributed force using the Fourier series is used. Then, the author utilized two boundary conditions (BCs) in each part, two continuity, and two equilibrium conditions on the interface to determine the eight unknown coefficients. Variation of deflection coefficients, radial moment coefficients, and shear coefficients along radial positions and angles was presented. However, some results are misleading. To investigate these inconsistencies, both null-field integral formulation and finite element method (FEM) using the ABAQUS are adopted to revisit this problem. In addition, two unclear issues in Ref. [1] are discussed. One is the simulation of concentrated load and the other is the operator of shear force.

2 Concentrated Load

In Adewale's paper [1], the author expanded the concentrated load to the Fourier series

$$P \approx P\left[\frac{1}{2} + \sum_{k=1}^{\infty} \frac{2\sin\dfrac{(2k-1)\pi}{2}}{(2k-1)\pi}\cos(2k-1)\theta\right], \quad 0 \le \theta \le \frac{\pi}{2} \tag{2}$$

By summing up the series of Eq. (2), the result converges to 1 as shown in Fig. 1, which does not show the behavior of the Dirac-delta function. The Dirac-delta function $\delta(x)$ should satisfy the identity as follows:

$$\int_{-\infty}^{\infty} \delta(x)dx = 1 \tag{3}$$

Equation (2) cannot satisfy Eq. (3) such that the strength of the concentrated loading is 1. The author seems to improperly transform the concentrated load to a circularly distributed one. If this load is distributed along an angle from 0 to $\pi/2$, the results of the deflection coefficient in Fig. 5 of Ref. [1] would be untrue.

3 Definition of Shear Force

For the clamped-free annular plate problems as shown in Fig. 2, the shear force on the inner circle is zero for the free boundary. Therefore, the author obtained the shear force

$$\left(\frac{\partial^3}{\partial r^3} - \frac{1}{r^2}\frac{\partial}{\partial r} + \frac{1}{r}\frac{\partial^2}{\partial r^2} - \frac{m^2}{r^2}\frac{\partial}{\partial r}\right)R_m(r)\bigg|_{r=a} = 0 \quad \text{shear force free} \tag{4}$$

According to the displacement of Eq. (1) and the definition of shear force operator in Szilard's book [3], the shear force can be derived as

$$\frac{\partial^3 R_m(r)}{\partial r^3} - \frac{1}{r^2}\frac{\partial R_m(r)}{\partial r} + \frac{1}{r}\frac{\partial^2 R_{m(r)}}{\partial r^2} + \frac{2m^2}{r^3}R_m(r) - \frac{m^2}{r^2}\frac{\partial R_m(r)}{\partial r} + (1-\nu)\left[\frac{m^2}{r^3}R_m(r) - \frac{m^2}{r^2}\frac{\partial R_m(r)}{\partial r}\right] \quad \text{for shear force} \tag{5}$$

where ν is the Poisson ratio. Equation (4) is unreasonable since it does not involve the Poisson ratio. In literature, many articles had reported the definition of shear force operator, e.g., Refs. [1–5]. We summarized the shear force operators in Table 1. After careful comparison, Adewale's shear force operator differs from the others and consequently, this difference may cause inconsistent results.

4 Alternative Derivation of the Analytical Solution Using the Null-Field Integral Formulation

The first boundary integral equations for the domain point can be derived from the Rayleigh–Green identity as follows [5,6]:

$$8\pi u(x) = U(\zeta,x) - \int_B U(s,x)v(s)dB(s) + \int_B \Theta(s,x)m(s)dB(s) - \int_B M(s,x)\theta(s)dB(s) + \int_B V(s,x)u(s)dB(s), \quad x \in \Omega \cup B \tag{6}$$

where B is the boundary of the domain Ω; $u(x)$, $\theta(x)$, $m(x)$, and $v(x)$ are the displacement, slope, normal moment, and effective shear force; and s and x are the source point and field point, respectively. The kernel function $U(s,x)$ in Eq. (6) is the fundamental solution that satisfies

$$\nabla^4 U(s,x) = 8\pi\delta(s-x) \tag{7}$$

Therefore, the fundamental solution can be obtained as follows:

Contributed by the Applied Mechanics Division of ASME for publication in the JOURNAL OF APPLIED MECHANICS. Manuscript received July 25, 2007; final manuscript received March 25, 2008; published online November 12, 2008. Review conducted by Subrata Mukherjee.

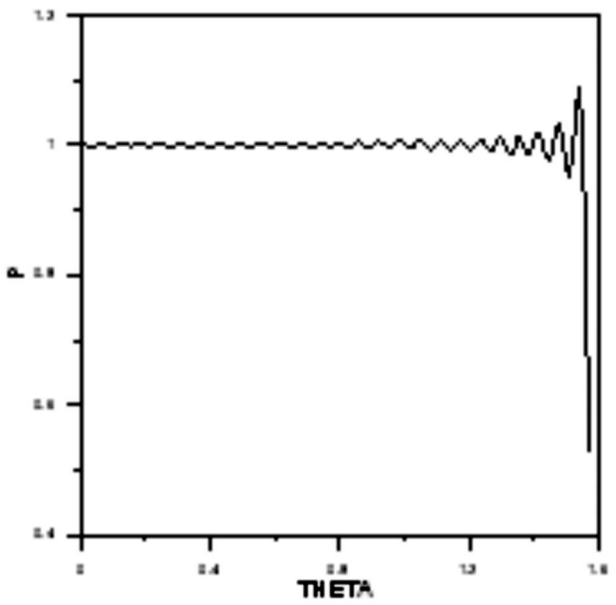

Fig. 1 Simulation of a concentrated force by Adewale's [1] (*M*=101).

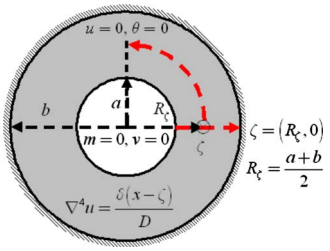

Fig. 2 Problem statement of an annular plate

$$U(s,x) = r^2 \ln r \tag{8}$$

where r is the distance between the source point s and field point x. The relationship among $u(x)$, $\theta(x)$, $m(x)$, and $v(x)$ is shown as follows:

$$\theta(x) = K_{\theta,x}(u(x)) = \frac{\partial u(x)}{\partial n_x} \tag{9}$$

Table 1 The definitions of the shear force (a) Szilard, (b) Leissa, (c) the present operator, and (d) Adewale

(a) Szilard [3]
$-D\left[\frac{\partial}{\partial r}\nabla_r^2 u + \frac{1-\nu}{r}\frac{\partial}{\partial \varphi}\left(\frac{1}{r}\frac{\partial^2 u}{\partial r \partial \varphi} - \frac{1}{r^2}\frac{\partial u}{\partial \varphi}\right)\right]$
(b) Leissa [4]
$-D\frac{\partial}{\partial r}(\nabla^2 u) + \frac{1}{r}\frac{\partial}{\partial \theta}\left[-D(1-\nu)\frac{\partial}{\partial r}\left(\frac{1}{r}\frac{\partial u}{\partial \theta}\right)\right]$
(c) Present operator [5]
$\frac{\partial \nabla_x^2 u}{\partial n_x} + (1-\nu)\frac{\partial}{\partial t_x}\left[\frac{\partial}{\partial n_x}\left(\frac{\partial u}{\partial t_x}\right)\right]$
(d) Adewale [1]
$\frac{\partial^3 R_m}{\partial r^3} - \frac{1}{r^2}\frac{\partial R_m}{\partial r} + \frac{1}{r}\frac{\partial^2 R_m}{\partial r^2} - \frac{m^2}{r^2}\frac{\partial R_m}{\partial r}$

$$m(x) = K_{m,x}(u(x)) = \nu \nabla_x^2 u(x) + (1-\nu)\frac{\partial^2 u(x)}{\partial^2 n_x} \tag{10}$$

$$v(x) = K_{v,x}(u(x)) = \frac{\partial \nabla_x^2 u(x)}{\partial n_x} + (1-\nu)\frac{\partial}{\partial t_x}\left[\frac{\partial}{\partial n_x}\left(\frac{\partial u(x)}{\partial t_x}\right)\right] \tag{11}$$

where $K_{\theta,x}(\cdot)$, $K_{m,x}(\cdot)$, and $K_{v,x}(\cdot)$ are the slope, moment, and shear force operators with respect to the point x; $\partial/\partial n_x$ is the normal derivative with respect to the field point x; $\partial/\partial t_x$ is the tangential derivative with respect to the field point x; and ∇_x^2 is the Laplacian operator. The first null-field integral equations can be derived by moving the field point x outside the domain as follows:

$$0 = U(\zeta,x) - \int_B U(s,x)v(s)dB(s) + \int_B \Theta(s,x)m(s)dB(s) - \int_B M(s,x)\theta(s)dB(s) + \int_B V(s,x)u(s)dB(s), \quad x \in \Omega^C \cup B \tag{12}$$

where Ω^C is the complementary domain of Ω. For the kernel function $U(s,x)$, it can be expanded in terms of degenerate kernel [2,5–7] in a series form as shown below:

$$U(s,x) = \begin{cases} U^I(R,\theta;\rho,\phi) = \rho^2(1+\ln R) + R^2 \ln R - \left[R\rho(1+2\ln R) + \frac{1}{2}\frac{\rho^3}{R}\right]\cos(\theta-\phi) \\ \quad - \sum_{m=2}^{\infty}\left[\frac{1}{m(m+1)}\frac{\rho^{m+2}}{R^m} - \frac{1}{m(m-1)}\frac{\rho^m}{R^{m-2}}\right]\cos[m(\theta-\phi)], \quad R \geq \rho \\ U^E(R,\theta;\rho,\phi) = R^2(1+\ln \rho) + \rho^2 \ln \rho - \left[\rho R(1+2\ln \rho) + \frac{1}{2}\frac{R^3}{\rho}\right]\cos(\theta-\phi) \\ \quad - \sum_{m=2}^{\infty}\left[\frac{1}{m(m+1)}\frac{R^{m+2}}{\rho^m} - \frac{1}{m(m-1)}\frac{R^m}{\rho^{m-2}}\right]\cos[m(\theta-\phi)], \quad \rho > R \end{cases} \tag{13}$$

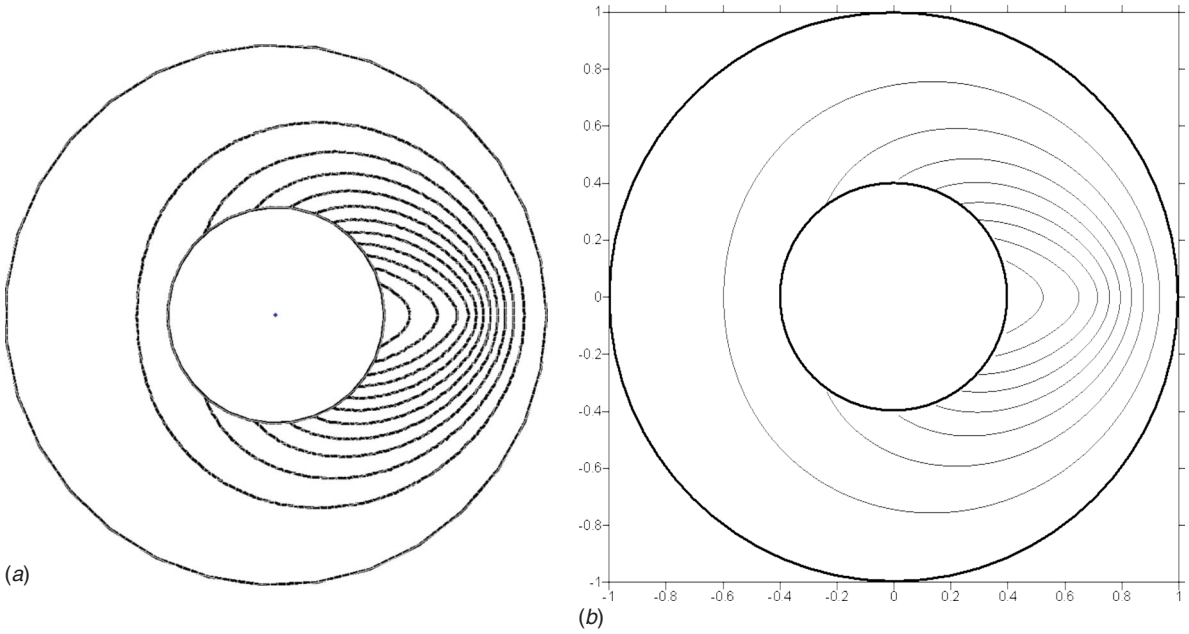

Fig. 3 Contour plots of the Green's function for the annular problem (a=0.4, b=1.0, R_ξ=0.7, D=1, ν=0.3). (a) Displacement contour by using the FEM (ABAQUS). (b) Displacement contour by using the present method (M=50).

where the superscripts I and E denote the interior and exterior cases of $U(s,x)$ kernel depending on the location of s and x. For the annular plate clamped at the outer edge and free at the inner edge, the unknown Fourier coefficients of m, v on the outer boundary and u, θ on the inner boundary can be expanded to

$$v(s) = a_0 + \sum_{n=1}^{M} (a_n \cos n\theta + b_n \sin n\theta), \quad s \in \text{outer boundary} \tag{14}$$

$$m(s) = \bar{a}_0 + \sum_{n=1}^{M} (\bar{a}_n \cos n\theta + \bar{b}_n \sin n\theta), \quad s \in \text{outer boundary} \tag{15}$$

$$\theta(s) = p_0 + \sum_{n=1}^{M} (p_n \cos n\theta + q_n \sin n\theta), \quad s \in \text{inner boundary} \tag{16}$$

$$u(s) = \bar{p}_0 + \sum_{n=1}^{M} (\bar{p}_n \cos n\theta + \bar{q}_n \sin n\theta), \quad s \in \text{inner boundary} \tag{17}$$

where a_0, a_n, b_n, $\bar{a}_0$, $\bar{a}_n$, $\bar{b}_n$, p_0, p_n, q_n, $\bar{p}_0$, $\bar{p}_n$, and $\bar{q}_n$ are the Fourier coefficients, and M is the number of Fourier series terms in real computation. By substituting all the Fourier coefficients of boundary densities and boundary conditions, the displacement field can be obtained as shown below:

$$8\pi u(x) = U(\zeta,x) - \int_B U(s,x)\left[a_0 + \sum_{n=1}^{M} (a_n \cos n\theta + b_n \sin n\theta)\right] dB(s) + \int_B \Theta(s,x)\left[\bar{a}_0 + \sum_{n=1}^{M} (\bar{a}_n \cos n\theta + \bar{b}_n \sin n\theta)\right] dB(s) - \int_B M(s,x) \times \left[p_0 + \sum_{n=1}^{M} (p_n \cos n\theta + q_n \sin n\theta)\right] dB(s) + \int_B V(s,x)\left[\bar{p}_0 + \sum_{n=1}^{M} (\bar{p}_n \cos n\theta + \bar{q}_n \sin n\theta)\right] dB(s), \quad x \in \Omega \cup B \tag{18}$$

where a_n, b_n, $\bar{a}_n$, $\bar{b}_n$, p_n, q_n, $\bar{p}_n$, and $\bar{q}_n$ (n=0,1,2,...) are solved in Ref. [7].

5 Results and Discussions

In order to verify the accuracy of Adewale's results, two alternatives, null-field approach and FEM using ABAQUS, are employed to revisit the annular problem. A concentrated load was applied at the radial center of the annular plate, as shown in Fig. 2. For the clamped-free boundary condition, Figs. 3(a) and 3(b) show the displacement contours for the Green's function by using FEM (ABAQUS) and the present method, respectively. Good agreement is obtained between our analytical solution and FEM result although Adewale [1] did not provide the displacement contour of his analytical solution. For comparison with the available results in Ref. [1], Fig. 4 shows the variation of deflection coefficients, moment coefficients, and shear force coefficients along radial positions or angles for different inner radii. It is also found that FEM results match well with our solution but deviates from Adewale's outcome [1].

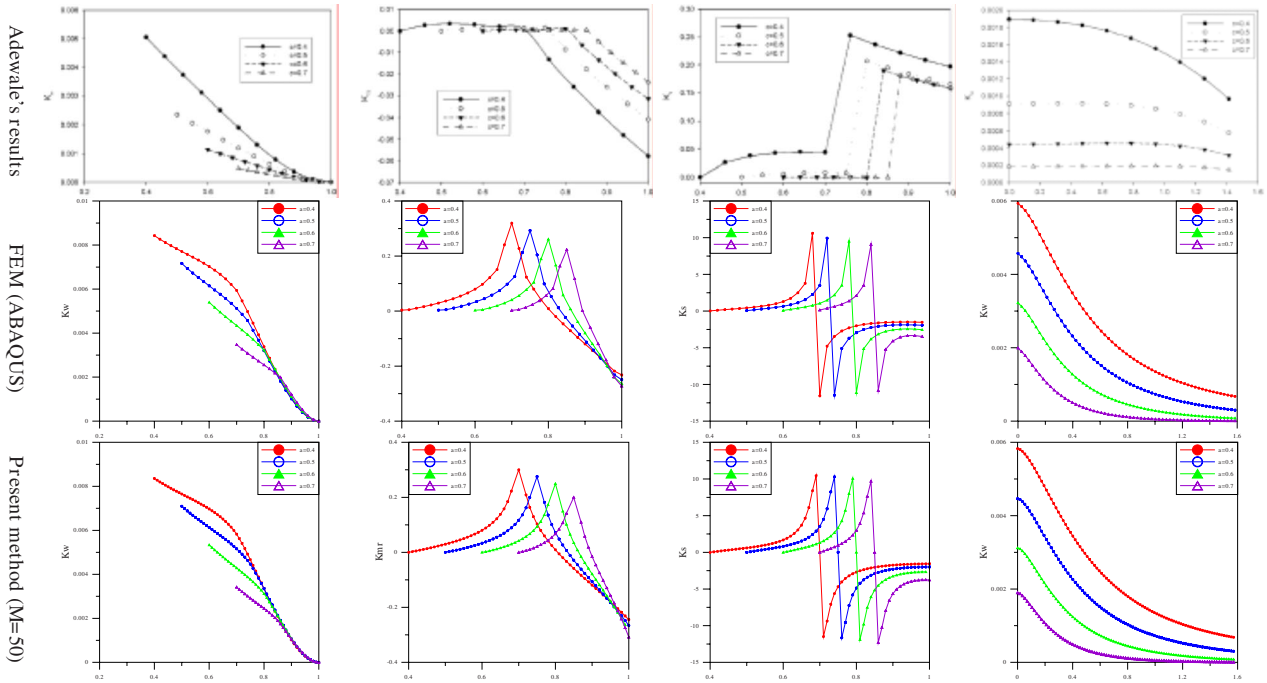

(a) Variation of deflection coefficients versus radial position

(b) Variation of moment coefficients versus radial position

(c) Variation of shear force coefficients versus radial position

(d) Variation of deflection coefficients versus radial angle

Fig. 4 Responses (b=1.0, R_ζ=0.7∼0.85, D=1, ν=0.3, $k_w = wD/P$, $k_{mr} = M_r D/P$, $k_s = M_s D/P$)

6 Concluding Remarks

To verify the accuracy of Adewale's results and to examine the response of the clamped-free annular plate subjected to a concentrated load, the null-field integral formulation was employed in solving this problem. The transverse displacement, moment, and shear force along the radial positions and angles for different inner radii were determined by using the present method in comparison with the ABAQUS data. Good agreements between our analytical results and those of ABAQUS were made but deviated from Adewale's data. The outcome of Adewale's results may not be correct.

References

[1] Adewale, A. O., 2006, "Isotropic Clamped-Free Thin Annular Circular Plate Subjected to a Concentrated Load," ASME J. Appl. Mech., **73**, pp. 658–663.

[2] Chen, J. T., Wu, C. S., and Lee, Y. T., 2007, "On the Equivalence of the Trefftz Method and Method of Fundamental Solutions for Laplace and Biharmonic Equations," Comput. Math. Appl., **53**, pp. 851–879.

[3] Szilard, R., 1974, *Theory and Analysis of Plates Classical and Numerical Methods*, Prentice-Hall, Englewood Cliffs, NJ.

[4] Leissa, A., 1993, *Vibration of Plates*, Acoustical Society of America, Melville, NY.

[5] Chen, J. T., Hsiao, C. C., and Leu, S. Y., 2006, "Null-Field Integral Approach for Plate Problems With Circular Boundaries," ASME J. Appl. Mech., **73**, pp. 679–693.

[6] Chen, J. T., Wu, C. S., and Chen, K. H., 2005, "A Study of Free Terms for Plate Problems in the Dual Boundary Integral Equations," Eng. Anal. Boundary Elem., **29**, pp. 435–446.

[7] Liao, H. Z., 2007, "Analytical Solutions for the Green's Functions of Laplace and Biharmonic Problems With Circular Boundaries," MS thesis, National Taiwan Ocean University, Taiwan.